Exploring Zeolite Chemistry with the Tools of Surface Science: Challenges, Opportunities and Limitations.

J. Anibal Boscoboinik[1*], Shamil Shaikhutdinov[2]

1. Center for Functional Nanomaterials, Brookhaven National Laboratory, Upton, New York 11973, USA.

2. Fritz-Haber-Institut der Max-Planck-Gesellschaft, Faradayweg 4-6, D-14195 Berlin, Germany

Abstract

The complexity of catalysts that the surface science community has been able to address has increased substantially in a systematic manner, starting with metal and oxide single crystal surfaces and evolving to an atomistic description of clusters and nanoparticles on well-defined, planar supports. The next step in adding complexity is now to address surfaces of porous oxide materials, in particular of zeolites, which are the most extensively used catalysts in the industry. The recently reported successful fabrication of well-ordered thin films, consisting of planar arrangement of aluminosilicate polygonal prisms on a metal substrate counting with highly acidic bridging hydroxyl groups on the surface, represents the limiting case of infinitely large pore and cages in zeolites. This model system allows one to study reactions catalyzed by zeolites using the toolkit of surface science. In this Perspective, we describe the zeolitic model system, with its virtues and limitations, as well as the challenges, opportunities and expectations for the future in modelling porous catalysts by a surface science approach.

The surface science community, in work pioneered by the groups of Somorjai and Ertl, [1-4] has successfully used simplified versions of industrial catalysts to provide insights on structure-reactivity relationships. By using so called "model" catalysts, the complexity of the catalyst can be reduced in order to disentangle structural, chemical and electronic effects in the reactions and elucidate reaction mechanisms. The study of catalytic systems by surface science methods began with metallic single crystal surfaces, and it has evolved systematically to the point that we now have a more detailed understanding, down to the sub-nanometer scale, of more complex systems such as clusters and nanoparticles on well-defined oxide surfaces. Even the remarkable effect of dopants and impurities in oxides may now be addressed. [5] While surface science has proven to be useful for a wide variety of catalytic processes, reactions on the most abundantly used catalysts, namely zeolites, remained a challenge due to the lack of suitable model systems mimicking zeolites. Basically, there is a simple reason for this. The vast majority of the surface science analytical techniques are only sensitive to exposed surfaces and, in the case of zeolites, the catalytically active surface is confined within cavities of the framework, rendering it inaccessible to techniques such as scanning probe microscopies and photoelectron spectroscopies. This has even led to the categorical claim that zeolite chemistry cannot be studied by surface science methods. [6]

There is an important motivation to understanding chemical reactions on zeolites, since they are the most used solid catalysts in the industry. [7-9] Among the many reactions they catalyze, perhaps the currently most important one is the catalytic cracking of crude oil in refineries around the globe. Other reactions include the conversion of alcohols into hydrocarbons and the selective catalytic reduction of NO_x, to name a few. These fascinating

three-dimensional crystalline aluminosilicates contain pores and channels of the size of small molecules (1-20 Å), also referred to as micropores or nanopores. They are structurally very diverse, with more than 200 different framework types already reported for zeolites and related materials (zeotypes), out of which about 40 have been found in nature, and the rest are the product of human ingenuity.[10] The number of framework types keeps growing every year and the possibilities seem endless with millions of hypothetical structures that have been proposed based reasonable geometrical constraints. [11]

For example, the unit cell of zeolite chabasite is shown in Figure 1a. All Si and Al atoms in the framework are covalently bound to four O atoms; that is, they have a tetrahedral coordination and hence are often referred to as T atoms. Conversely, each O atom is bound to two T atoms of the structure, thus yielding a TO_2 stoichiometry. Given the trivalent nature of Al, the tetrahedral coordination gives rise to one negative charge in the zeolite framework for each Al atom. This can also be expressed as $Al_xSi_{(1-x)}O_2^{x-}$, in order to distinguish Si from Al, where "*x"* is the Al molar ratio:

$$x = \frac{n_{Al}}{n_{Al} + n_{Si}}$$

that varies between *x = 0* and *x = 0.5*. [12] (This notation differs from the one commonly used within the zeolite community in which the Si/Al ratio is reported. We will use both notations in this paper). This negative charge is usually compensated by a cation bound to one of the O atoms surrounding Al. For the chabasite zeolite shown in Figure 1a, the cation species that compensates the framework charge is a proton, giving rise to hydroxo species also known as a "bridging hydroxyl", Si-$(OH)_{br}$-Al. While many different cations (often alkali metals) can provide such charge compensation, the case of the proton is of great importance for acid-base catalysis, since it provides the zeolite with a very strong Brönsted acid site, which is

responsible for catalytic reactions such as the cracking of hydrocarbons and the methanol to hydrocarbons conversion. Considering this and the fact that a proton is the simplest cation, we will concentrate our attention on this case for now. Note also that we deal here with models for the interior of the zeolite pores, and not the outer surface of zeolite crystals. The external surface of zeolites has been studied for example by atomic force microscopy to significant level of detail such that now mechanisms of zeolite growth can be addressed using this strategy, [13] and even molecules on the surface of zeolite crystallites could be imaged [14].

What criteria should an experimental model system fulfill in order to be considered suitable for surface science studies of zeolites? Certainly, the model must be a crystalline aluminosilicate framework, with Si and Al atoms each bound to four O atoms, that exposes the active site at the surface to be accessible to the method used. The active site should, of course, show the same chemical behavior as that found on real catalysts. Additionally, since zeolites are electrical and thermal insulators and many surface science techniques are based on charged species (electrons and ions), it would be advantageous to prepare the aluminosilicate on a metallic substrate as a film, but making the film thin enough to provide electrical conductivity of the samples. However, the interaction with the metallic substrate should be minimized, otherwise it may influence the surface chemistry of the active species. Additionally, the metallic support should be fully covered by the zeolite film or, alternatively, the metallic substrate itself should not catalyze any reaction involving the molecules that will be interacting with, or produced at, the zeolite surface.

There were several attempts in the past to prepare model systems for zeolites. [15] However, the synthesis of well-defined crystalline thin zeolite films remained a challenge for many years. Important progress towards making flat thin aluminosilicates was accomplished

by Stacchiola et al. [16], by preparing the first ever reported well-defined ordered two-dimensional aluminosilicate structure on a metallic substrate, in that case on Mo(112). However, the ultimate goal of creating a system with highly acidic protons was not reported until recently in a short communication. [17] This film was synthesized based on a preparation of silica (SiO_2) bilayer structure first reported by Löffler et al. [18]. Using Si and Al co-deposition, some of the Si atoms in the silica film can be replaced by Al, thus resulting in aluminosilicate films. The film structure is shown in Fig. 1b. It is composed of a two-dimensional arrangement of polygonal prisms, where the T atoms are located at the vertices of the polygons and the O atoms at the edges. The vast majority of these polygons are hexagonal prisms and thus we will refer to this structure as “2dH” (two-dimensional hexagonal), following the notation established previously. [19] The surface symmetry was determined by low energy electron diffraction (LEED), and Si and Al contents were determined by x-ray photoelectron spectroscopy. [17, 20] While LEED shows long-range ordering (i.e. crystallinity) regardless of the Al content, scanning tunneling microscopy (STM) images show local variations in the crystallinity at the atomic scale. Figure 2 shows STM images and corresponding LEED patterns for aluminosilicate films with ratios (a) Si/Al = 7.3 and (b) Si/Al = 1.8. It is only by STM, which shows structural details down to the atomic scale, that the presence of other ring sizes was identified. [21] The distribution of polygon sizes depends of the Al content, although only for Si/Al ratios lower than 3 (i.e. $x > 0.25$) a significant population of ring sizes other than the hexagon can be observed. For $x < 0.25$, Al containing domains are separated from the all-Si domains by boundaries containing 5- and 7-membered rings, while all rings within the domains are 6-membered (Figures 2a and 2b). This can be seen in figure 2b, where the domain on the left contains Al and Si in tetrahedral positions while for the domain on the right the only T species are Si atoms

(see ref. [17] for details). The observation that the Al atoms are not randomly distributed across the surface, but segregate into domains, is not trivial, since it contradicts Dempsey's statement [22] based on electrostatic considerations, that Al atoms arrange in zeolitic structures as far as possible from each other. In contrast, the strain induced by defects (an Al atom can be seen as a defect) may be minimized when the defects are located near each other. As a result of this delicate balance, Al-O-Si-O-Al linkages can be favorable under certain conditions, in particular within four-membered silica rings, [23] which are definitely present in our films, as they connect the top and bottom layers. When the Al content reaches x = 0.25, the bottom layer of the framework has reached is maximum capacity within the constraints of Lowenstein's rule, [24] that states that Al—O—Al linkages in zeolitic frameworks are forbidden. It is only then that Al atoms begin populating the top layer of the framework and form bridging hydroxyls, as it will be described below. Figure 2c also shows that for $x > 0.25$ a larger spread of ring sizes can be observed. In fact, both crystalline and amorphous regions can be present on surface. However, the distribution of ring sizes in the amorphous regions is not random and, when compared to a vitreous silica bilayer, [25] the aluminosilicate films exhibit an increased population of even-numbered rings (such as 4- and 8-), which is, again, related to Lowenstein's rule. For a more thorough analysis of ring distributions the reader is referred to ref. [21]. Is worth noting that while the amorphous (vitreous) phase is observed in pure SiO_2 bilayer films prepared under the same conditions, the aluminosilicate films always exhibit the crystalline structure for low Al contents ($x < 0.25$) [26]. Noteworthy, a closely related layered structure, with "$x = 0.5$", consisting of intercalated layers of a 5 Å thick aluminosilicate structure and Ba^{2+} cations had been previously described by Yoshiki et al. [27]

The most compelling evidence of the proposed atomic structure shown in Fig. 1b came

from infrared reflection-absorption spectroscopy (IRAS) studies. In the phonon region, a strong peak between 1300 and 1260 cm^{-1} and another one between 692 and 702 cm^{-1} are observed depending on the Al content, which correspond to vibrations in the frameworks as schematically shown in Fig. 3. The high-frequency peak gradually shifts towards lower frequencies, whereas low-frequency peak becomes broader as the Al content increases.

In addition, IRAS results unambiguously show the presence of bridging hydroxyls on the film surface upon hydroxylation resulting in a signal at 3594 cm^{-1}. Henceforth, we will refer to the hydroxylated film as H-2dH. The spectrum in Figure 4a shows that the film exhibits hydrogen-deuterium exchange after D_2O exposure to the H-2dH surface, thus resulting in the ν(OD) peak at 2653 cm^{-1}. The acidic properties of bridging OH (OD) were examined by adsorption of different probe molecules commonly used for zeolites.

Weak bases such as CO and C_2H_4 form a complex with the proton of the hydroxyl group without breaking the O—H bond. The formation of the complex induces a red-shift in the O—H stretching mode, and this shift is proportional to the acidity of the proton. This is a widely used strategy for measuring the acidity of solid acids, including zeolites. [28, 29] Figure 4c shows the difference spectrum for CO adsorbed on H-2dH, where a red shift of 379 cm^{-1} is observed. Accordingly, Figure 4b shows a red shift of 243 cm^{-1} induced by CO on the bridging OD vibration, as expected from analysis of the reduced masses. Note also a peak at 2183 cm^{-1} appears in spectra 4b and 4c. This corresponds to the ν(CO) stretching vibration, which is blue-shifted 40 cm^{-1} with respect to gas phase CO and also gives an indication of the acidity of the bridging OH and OD groups that agrees with the one found based on the ν(OH) and ν(OD) shifts. The other weak base used as a probe molecule was ethylene. Figure 5a shows a spectrum of a D-2dH film that, aside from the bridging OD groups (2655 cm^{-1}), also contains

silanol (Si-OD) groups (2763 cm^{-1}) arising from defects on the surface. [30] This surface allows us to compare the acidities of the two different types of OD groups. Figures 5b and 5c correspond to increasing doses of C_2H_4 on the surface, where in Fig. 5b ~50% of the bridging OD groups have been "titrated" and the saturation point is reached in 5c. Here the peak at 2330 cm^{-1} corresponds to the OD stretching vibration in the complex. The broadening and increase in intensity upon formation of the complex is common to H- bonded complexes and has also been observed in zeolites. [31] The peak at 992 cm^{-1} corresponds to C-H wagging modes. It is important to emphasize here, as evident from spectra 5b and 5c, that the Si-OD group does not form any complex with C_2H_4 because of its low acidic character.

It is noteworthy that C_2H_4 is used as feedstock in the olefin polymerization reaction, [32] another important chemical process catalyzed by acidic zeolites, where the ethylene-bridging OH complex is presumably the precursor state for this catalytic process.

Figure 6 shows a plot of $\Delta\nu_{(O—H)}$ shifts induced by CO and C_2H_4 for a variety of zeolites and zeotypes taken from the literature and for our H-2dH films [19]. As it can be seen in this figure, the acidity of the model system is similar to, and even higher than some of the catalytically active zeolites used in the industry. This is important, since larger shifts have been correlated with higher catalytic activity [33, 34]. This finding indicates that the prepared model system may potentially be active, thus allowing further mechanistic studies to be carried out. Adsorption of strong bases, ammonia and pyridine, resulted in the abstraction of the proton from the bridging hydroxyl groups to form ammonium and pyridinium ions, respectively, i.e. in full agreement with what has previously been found in zeolites. [19]

As an example of adsorption studies with more catalytically relevant molecules, we address here the interaction of an aluminosilicate film with methanol which is one of the reactants in the

methylation of olefins. [35, 36] Figure 7 shows a series of IRA-spectra after CD_3OD adsorption at ~ 100 K followed by heating to the temperatures as indicated. (Note that the presented spectra are referenced to the spectrum taken before the methanol exposure, that is a positive (negative) $\Delta R/R$ signal is attributed to disappearance (respectively, formation) of surface species). The peak at 3594 cm^{-1} of the bridging OH group in the film disappears upon physical condensation of methanol that typically occurs at this low temperature (~ 100 K). On heating to 150 K (Fig. 7a), weakly bonded methanol desorbs from the surface, [37] albeit some molecules remain on the surface as judged by the IRAS bands at 2500 – 2000 cm^{-1},[38] which intensity reduces upon heating to 200 K (7b) and further to 250 K (7c). Only a C—D stretching vibration at 2073 cm^{-1} remains on the surface, shifting to 2092 cm^{-1} at 250 K and ultimately disappears at 300 K, possibly arising from decomposition products of methanol. Concomitantly, a peak appears at 2653 cm^{-1}, corresponding to a bridging OD group, whereas the original OH peak at 3594 cm^{-1} does not recover upon methanol desorption. These results clearly indicate interaction of CD_3OD methanol with bridging OH, which is accompanied by the H/D exchange reaction. An adsorption scheme for CD_3OD on bridging hydroxyls in H-Chabasite was previously proposed by Svelle et al. [36] on the basis of DFT calculations, in which the hydrogen coming from the methanol hydroxyl and the one of the bridging hydroxyl are indistinguishable in the adsorption complex. Our results agree well with this scheme, and provide further evidence that these aluminosilicate films are, indeed, well-suited for studying surface chemistry of zeolites at atomic level.

It should be emphasized that this model system is different from the thriving family of two-dimensional zeolites, described in detail in a recent review, [39] which can be produced as layered forms of three-dimensional ones only limited in thickness to one unit cell. [40, 41] At

variance, the model system described here is not a truncated framework that would result in surfaces with dangling bonds and/or silanol groups. Instead, the H-2dH zeolite film is a standalone structure with all bonds covalently saturated within the framework, and only weakly interacting with the metal support.

Certainly, the suggested model system has some limitations which we would like to address here in more detail.

Interaction of the metallic substrate with the zeolite framework. Although bridging hydroxyls in the current model have shown a chemical behavior similar to those in three-dimensional zeolites in terms of the interaction with probe molecules, one cannot exclude interaction between the aluminosilicate framework and a metallic substrate. While there are no strong bonds between them, the presence of electrostatic interactions between the framework and the metal cannot be discarded. In fact, it is very likely that the framework charge at the bottom layer of the structure is compensated by the metal surface, which would be consistent with the preferential location of Al at the bottom layer and hence the absence of bridging hydroxyl groups at low Al content, $x < 0.25$ (i.e.: Si/Al > 3). While this might or might not have an effect in the chemistry of the bridging hydroxyls that do exist for $x > 0.25$ (Si/Al < 3), eliminating this interaction, by further decoupling the aluminosilicate framework from the metal substrate, would provide a more reliable model system.

Effects of the surface curvature and micropores*.* While the lack of micropores in the current model system can be seen as a disadvantage, since it does not allow to study size-selectivity effects commonly observed in 3D-zeolites, there are many advantages of having a planar structure. In real zeolites, even in the ideal case of a structure with no defects, there are many factors that will affect the chemistry, such as mass and heat transport limitations, acidity

of the site and van der Waals interactions of the involved reactants, intermediates and products with the walls of the pore. This complexity is tremendously reduced in the case of the planar system, in which there are no transport limitations and there is no wall on the opposite side of the active site for the involved molecules to interact with. Thus, this approach will only give information about the active site. The Sauer group has provided a useful description of the influence of the curvature on the acidity of the bridging hydroxyl, as measured by the heat of adsorption calculated using the DFT+D approach, comparing H-2dH film with H-chabasite and separating the contribution of dispersion forces to the heat of adsorption. [19] It was found that, for weak bases CO and C_2H_4 interacting with bridging hydroxyls, the heat of adsorption is higher for OH_{br} in H-chabasite than for OH_{br} in H-2dH. However, the case of adsorption on H-chabasite also shows much higher dispersion forces when compared to H-2dH, likely due to the van der Waals interactions of CO and C_2H_4 with the pore walls in chabasite, which is greatly reduced in the planar case. This translates then in the actual interaction between the probe molecules and the bridging OH, being stronger for H-2dH, in agreement with the conclusions based on the spectral shifts in the OH vibrational frequency upon adsorption of the weak base molecules, both in experiment and in theory. The increased acidity of H-2dH is likely related to a curvature effect. Indeed, in the planar system Si—O—Al angles are closer to 180° than in H-Chabasite, and that strain probably induces a weaker O—H bond, in agreement to the longer O—H bond length found as well in the DFT calculations for H-2dH.

While the lack of porosity, which is one of the most important features of zeolites, would seem like a disadvantage in the two-dimensional system described here, analysis of possible differences between the planar zeolite and three-dimensional ones could give valuable information about effects of the pores on the chemistry.

Effect of Al/Si ratio. One of the downsides of the current preparation of H-2dH is that bridging hydroxyls are found on the surface of the model system only for Si/Al < 3 (x > 0.25), which is very different from the real zeolite catalysts where typical Si/Al ratios are significantly higher. This is due to the fact that, in the current model, Al at low contents preferentially occupies sites in the bottom layer, which could be related to the effective charge compensation from the metal support. It is only when the bottom layer becomes saturated with Al, to the extent governed by Lowenstein's rule, that the second layer begins to populate, and bridging hydroxyls are formed as shown by IRAS. Therefore, new preparation methods that drive Al to the top layer should be explored in order to properly match the Si/Al ratios found in real catalysts.

Reactivity of H-2dH zeolite film. While IRAS experiments using probe molecules to gauge the chemistry of the bridging hydroxyls revealed that they truly behave like in real zeolites, the experiments were so far performed at low pressures, at which structural changes are negligible. The next step is to find the conditions, of pressure and temperature, at which specific reactions take place, for chemical processes of interest in catalysis. In order to induce chemical transformations, higher pressures are needed and efforts are currently being made in this direction.

Other model systems. In the studies carried out so far on the model system, the active site is an acidic bridging hydroxyl group and this is indeed the active site for many acid-base reactions. In catalysis applications however, there are many other systems involving zeolites in which the active sites consist of other species. The proton can be replaced by other cations to stabilize the framework charge. An important example is the case in which transition metals such as Cu or Fe are used, for example for the selective catalytic reduction of NO_x gases

resulting from combustion processes. [42] Cu, Zn-zeolites have also been shown to be active for the water-gas shift reaction. [43] Additionally, zeolites are often used as a support for metal clusters, with both the zeolite and metal particles playing an important role in the reaction. This kind of systems can, in principle, be studied using the aluminosilicate film on top of which metals can be deposited. Conversely, “inverse” model systems can be fabricated by preparing aluminosilicate frameworks only partially covering a metallic support of interest. In fact, we have recently reported the preparation of a system with this feature, by preparing an aluminosilicate bilayer structure leaving exposed about 50% of the Ru(0001) surface, [44] which could be interesting to model a Fischer-Tropsch catalyst consisting of Ru particles on zeolites. [45]

Final remarks.

After a many years of effort, a well-defined aluminosilicate film that exposes bridging hydroxyl groups similar to the ones found in zeolites is available for model system surface science studies of chemical processes catalyzed by the Brönsted acid form of these fascinating porous solids. This will allow the future investigation of some of the most important reactions in the industry, such as the methanol to hydrogen conversion and cracking of hydrocarbons, among many others. While ultra-high vacuum studies of the H-2dH model system have shown the same chemical behavior as zeolites when interacting with weak and strong bases, the challenge of carrying out actual chemistry on this film still lies ahead of us.

Slight modifications of this model system allow us as well to envision the study of reactions other than those catalyzed by Brönsted acid sites when the cationic species neutralizing the charge in the framework are not protons, but metal cations. This is the case for example of the selective catalytic reduction of NO_x which can be catalyzed by Fe- or Cu-

containing zeolites.

While the fabricated zeolite films do count with the basic requirements of a zeolite model system, synthetic methodologies for creating different structures, perhaps even borrowing concepts from the zeolite community using structure directing agents to modulate pore sizes or using layered zeolites such as MCM-22 (or layered zeolite precursors) as starting materials for the synthesis, provide interesting alternatives which could also help assess the influence of structural parameters in the chemistry of zeolites.

Another interesting unexplored avenue to change the topology is the introduction of other elements to the framework known to have an effect in the ring size distributions, such as Ge, Ga, which are known to favor 4-membered rings. Also, other microporous systems of catalytic relevance such as aluminophosphates (ALPOs) or silicoaluminophosphates (SAPOs) could be explored.

All in all, this is just the beginning of an exciting journey within surface science and while there are still limitations and challenges to overcome, there are many opportunities and approaches that can be taken to address, from a fundamental point of view, some of the most important catalytic reactions in the industry, which involve the use porous materials.

Acknowledgements

We gratefully thank Prof. H.-J. Freund and all our coworkers cited in the references, in particular the theory group of Prof. J. Sauer, for their tremendous contribution to the work presented here. J.A.B thanks the A. von Humboldt Foundation and the Center for Functional Nanomaterials at BNL, under DOE contract No. DE-AC02-98CH10886.

References

1. Somorjai, G. A.; Park, J. Y. *Surface Science* **2009,** 603, (10-12), 1293-1300.
2. Ertl, G. *Surface Science* **1994,** 299, (1-3), 742-754.
3. Somorjai, G. A.; Li, Y. M. *Topics in Catalysis* **2010,** 53, (5-6), 311-325.
4. Ertl, G. *Angewandte Chemie-International Edition* **2008,** 47, (19), 3524-3535.
5. Freund, H.-J.; Shaikhutdinov, S.; Nilius, N. *Topics in Catalysis* **2014,** 57, (10-13), 822-832.
6. Haw, J. F. *Physical Chemistry Chemical Physics* **2002,** 4, 5431-5441.
7. Martínez, C.; Corma, A. *Coord. Chem. Rev.* **2011,** 255, (13-14), 1558-1580.
8. Yilmaz, B.; Müller, U. *Top. Catal.* **2009,** 52, 888-895.
9. Corma, A. *Chemical Reviews* **1995,** 95, (3), 559-614.
10. Baerlocher, C.; McCusker, L. B., (Accessed 07/01/2014).
11. Foster, M. D.; Treacy, M. M. J. *A Database of Hypothetical Zeolite Structures: http://www.hypotheticalzeolites.net*, (accessed 08/17/14).
12. Baerlocher, C.; McCusker, L. B.; Olson, D. H., *Atlas of Zeolite Framework Types*. Sixth ed.; Elsevier B. V.: Amsterdam, 2007.
13. Lupulescu, A. I.; Rimer, J. D. *Science* **2014,** 344, (6185), 729-732.
14. Weisenhorn, A. L.; Mac Dougall, J. E.; Gould, S. A. C.; Cox, S. D.; Wise, W. S.; Massie, J.; Maivald, P.; Elings, V. B.; Stucky, G. D.; Hansma, P. K. *Science* **1990,** 247, (4948), 1330-1333.
15. Shaikhutdinov, S.; Freund, H. J. *Chemphyschem* **2013,** 14, (1), 71-77.
16. Stacchiola, D.; Kaya, S.; Weissenrieder, J.; Kuhlenbeck, H.; Shaikhutdinov, S.; Freund, H.-J.; Sierka, M.; Todorova, T. K.; Sauer, J. *Angew. Chem. Int. Ed.* **2006,** 45, 7636-7639.
17. Boscoboinik, J. A.; Yu, X.; Yang, B.; Fischer, F. D.; Włodarczyk, R.; Sierka, M.; Shaikhutdinov, S.; Sauer, J.; Freund, H.-J. *Angew. Chem. Int. Ed.* **2012,** 51, 6005-6008.
18. Löffler, D.; Uhlrich, J. J.; Baron, M.; Yang, B.; Yu, X.; Lichtenstein, L.; Heinke, L.; Büchner, C.; Heyde, M.; Shaikhutdinov, S.; Freund, H.-J.; Wlodarczyk, R.; Sierka, M.; Sauer, J. *Phys. Rev. Lett.* **2010,** 105, 146104.
19. Boscoboinik, J. A.; Yu, X.; Emmez, E.; Yang, B.; Shaikhutdinov, S.; Fischer, F. D.; Sauer, J.; Freund, H.-J. *Journal of Physical Chemistry C* **2013,** 117, (26), 13547-13556.
20. Boscoboinik, J. A.; Yu, X.; Yang, B.; Fischer, F. D.; Włodarczyk, R.; Sierka, M.; Shaikhutdinov, S.; Sauer, J.; Freund, H.-J. *Angew. Chem.* **2012,** 124, (24), 6107-6111.
21. Boscoboinik, J. A.; Yu, X.; Yang, B.; Shaikhutdinov, S.; Freund, H.-J. *Microporous and Mesoporous Materials* **2013,** 165, 158-162.
22. Dempsey, E. *Journal of Catalysis* **1974,** 33, (3), 497-499.
23. Schroeder, K. P.; Sauer, J. *The Journal of Physical Chemistry* **1993,** 97, (25), 6579-6581.
24. Lowenstein, W. *Am. Mineral.* **1954,** 39, 92.
25. Lichtenstein, L.; Büchner, C.; Yang, B.; Shaikhutdinov, S.; Heyde, M.; Sierka, M.; Włodarczyk, R.; Sauer, J.; Freund, H.-J. *Angewandte Chemie* **2012,** 124, (2), 416-420.
26. Büchner, C.; Lichtenstein, L.; Yu, X.; Boscoboinik, J. A.; Yang, B.; Kaden, W. E.; Heyde, M.; Shaikhutdinov, S. K.; Włodarczyk, R.; Sierka, M.; Sauer, J.; Freund, H.-J. *Chemistry – A European Journal* **2014,** 20, (30), 9176-9183.
27. Yoshiki, B.; Matsumoto, K. *J. Am. Ceram. Soc.* **1951,** 34, 283–286.
28. Lamberti, C.; Zecchina, A.; Groppo, E.; Bordiga, S. *Chem. Soc. Rev.* **2010,** 39, 4951-5001.
29. Bordiga, S.; Regli, L.; Cocina, D.; Lamberti, C.; Bjørgen, M.; Lillerud, K. P. *J. Phys. Chem. B* **2005,** 109, 2779-84.

30. Yang, B.; Kaden, W. E.; Yu, X.; Boscoboinik, J. A.; Martynova, Y.; Lichtenstein, L.; Heyde, M.; Sterrer, M.; Wlodarczyk, R.; Sierka, M.; Sauer, J.; Shaikhutdinov, S.; Freund, H.-J. *Phys. Chem. Chem. Phys.* **2012,** 14, (32), 11344-11351.
31. Makarova, M. A.; Ojo, A. F.; Karim, K.; Hunger, M.; Dwyer, J. *J. Phys. Chem.* **1994,** 98, 3619-3623.
32. Spoto, G.; Bordiga, S.; Ricchiardi, G.; Scarano, D.; Zecchina, A.; Borello, E. *J. Chem. Soc., Faraday Trans.* **1994,** 90, 2827.
33. Lavalley, J.-C.; Jolly-Feaugas, S.; Janin, A.; Saussey, J. *Mikrochim. Acta Supp.* **1997,** 14, 51-56.
34. Umansky, B.; Engelhardt, J.; Hall, W. K. *J. Catal.* **1991,** 127, 128-140.
35. Hill, I. M.; Al Hashimi, S.; Bhan, A. *Journal of Catalysis* **2012,** 285, (1), 115-123.
36. Svelle, S.; Tuma, C.; Rozanska, X.; Kerber, T.; Sauer, J. *Journal of the American Chemical Society* **2009,** 131, (2), 816-825.
37. Nishimura, S. Y.; Gibbons, R. F.; Tro, N. J. *The Journal of Physical Chemistry B* **1998,** 102, (35), 6831-6834.
38. Shimanouchi, T. *Tables of Molecular Vibrational Frequencies Consolidated Volume I, National Bureau of Standards* **1972**, 1-160.
39. Roth, W. J.; Nachtigall, P.; Morris, R. E.; Čejka, J. *Chemical Reviews* **2014,** 114, (9), 4807-4837.
40. Tsapatsis, M. *AIChE Journal* **2014,** 60, (7), 2374-2381.
41. Zhang, X.; Liu, D.; Xu, D.; Asahina, S.; Cychosz, K. A.; Agrawal, K. V.; Al Wahedi, Y.; Bhan, A.; Al Hashimi, S.; Terasaki, O.; Thommes, M.; Tsapatsis, M. *Science* **2012,** 336, (6089), 1684-1687.
42. Brandenberger, S.; Kröcher, O.; Tissler, A.; Althoff, R. *Catalysis Reviews* **2008,** 50, (4), 492-531.
43. Regina Oliveira de Souza, T.; Modesto de Oliveira Brito, S.; Martins Carvalho Andrade, H. *Applied Catalysis A: General* **1999,** 178, (1), 7-15.
44. Boscoboinik, J. A.; Yu, X.; Shaikhutdinov, S.; Freund, H.-J. *Microporous and Mesoporous Materials* **2014,** 189, (0), 91-96.
45. Cheng, K.; Kang, J.; Huang, S.; You, Z.; Zhang, Q.; Ding, J.; Hua, W.; Lou, Y.; Deng, W.; Wang, Y. *ACS Catal.* **2012,** 2, (3), 441-449.

Figure 1

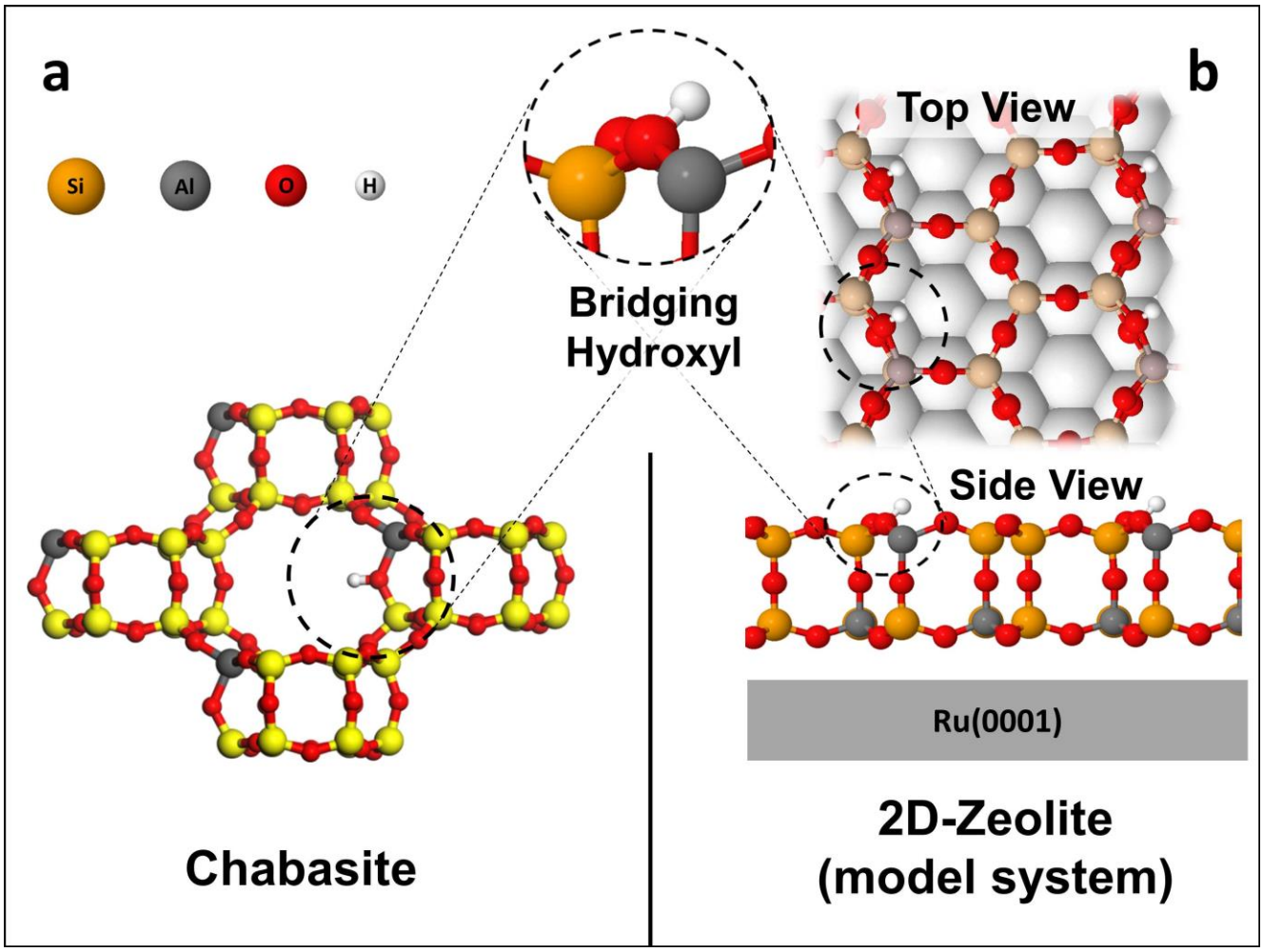

Figure 1. (a) Zeolite Chabasite in its protonated form. (b) Protonated form of the 2-dimensional zeolite model system showing the bridging hydroxyl group. The top and side views of the structure of the model system are shown.

Figure 2

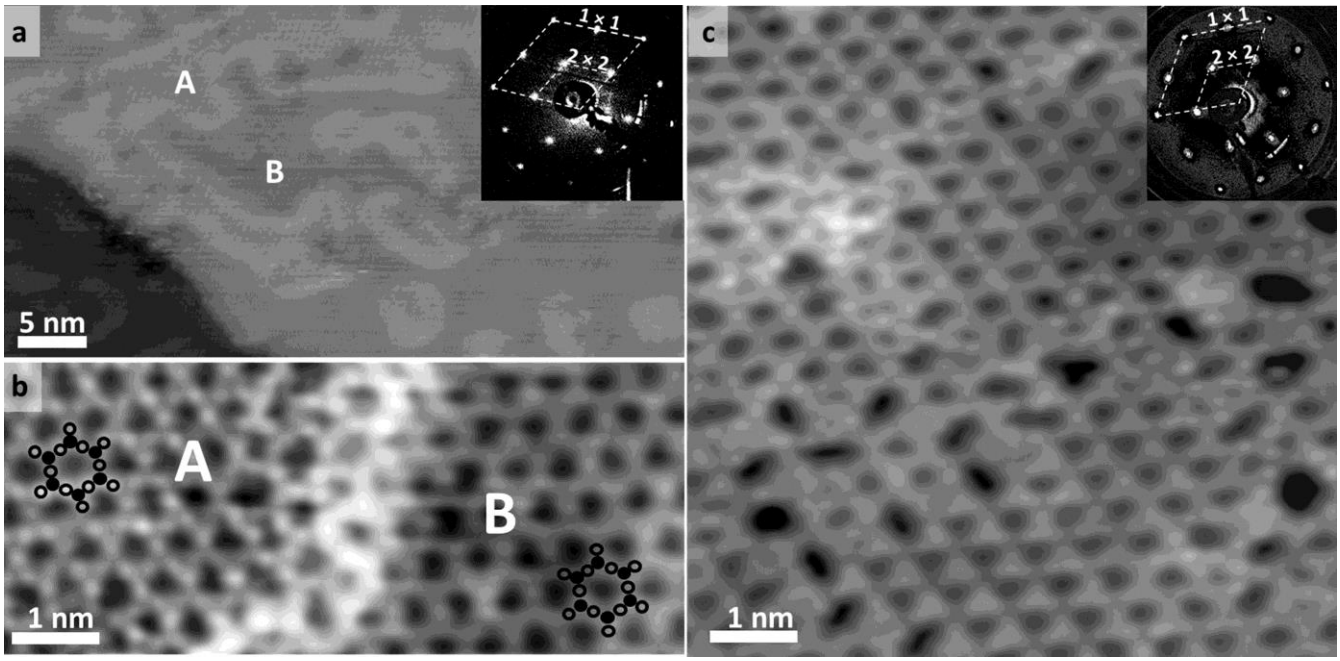

Figure 2. STM images for aluminosilicate bilayer frameworks with different compositions. Figure (a) shows a long range image of a framework with stoichiometry $Al_{0.12}Si_{0.88}O_2$ (Si/Al = 7.3) and (b) shows close up of the same film with atomic resolution, the location of tetrahedral (black circles) and oxygen (open circles) atoms is indicated for two of the rings. Figure (c) corresponds to a framework with stoichiometry $Al_{0.36}Si_{0.64}O_2$ (Si/Al = 1.8), where both crystalline and amorphous regions are imaged. (a) and (c) also show insets with the LEED patterns of these films, showing the long range (2 × 2) structure. Figure adapted from ref. [17] and [21].

Figure 3

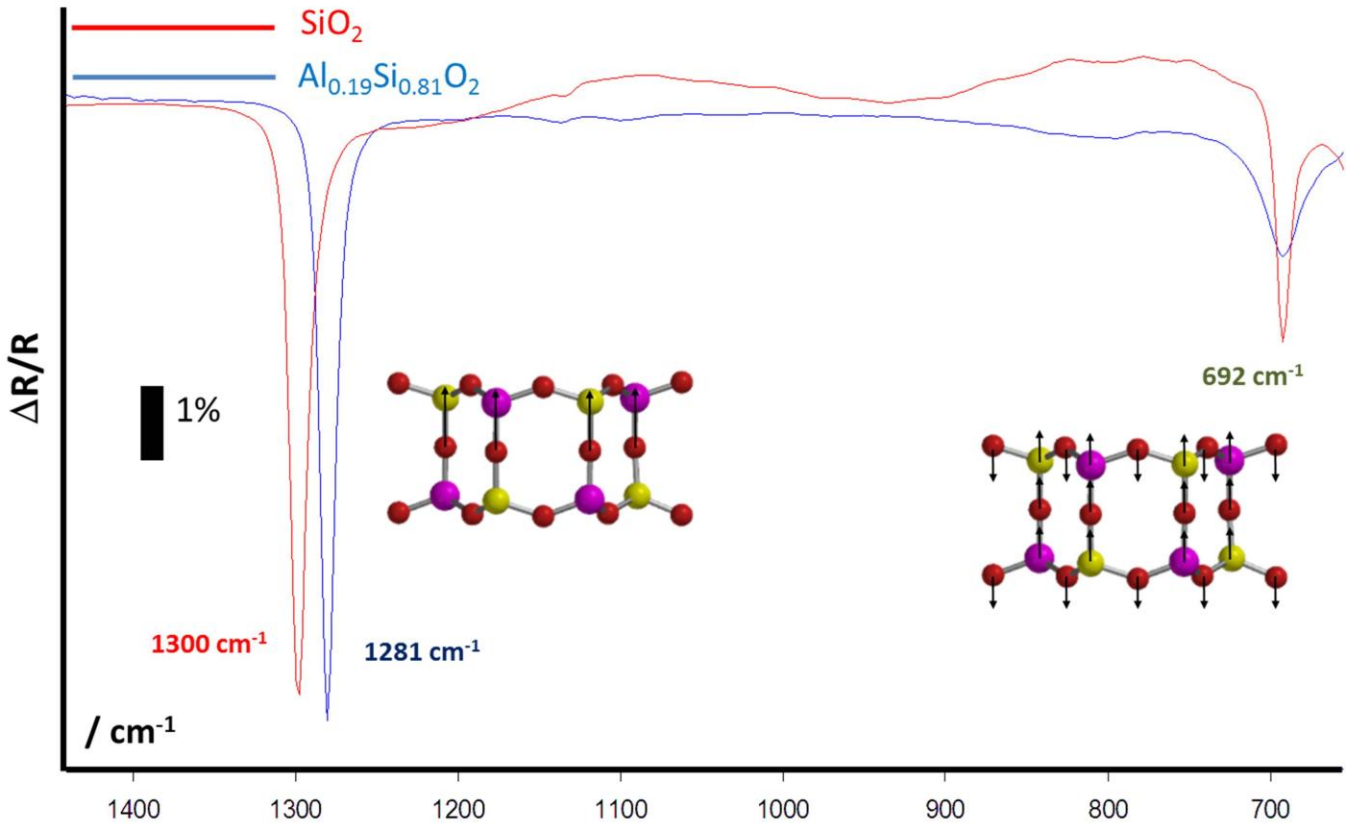

Figure 3. IRAS spectra for films with stoichiometries SiO_2 (red line) $Al_{0.19}Si_{0.81}O_2$ (blue line) showing characteristic phonon vibrations in the framework.[17] The schematics of the phonon vibrations are also shown for the high and low frequency peaks.

Figure 4

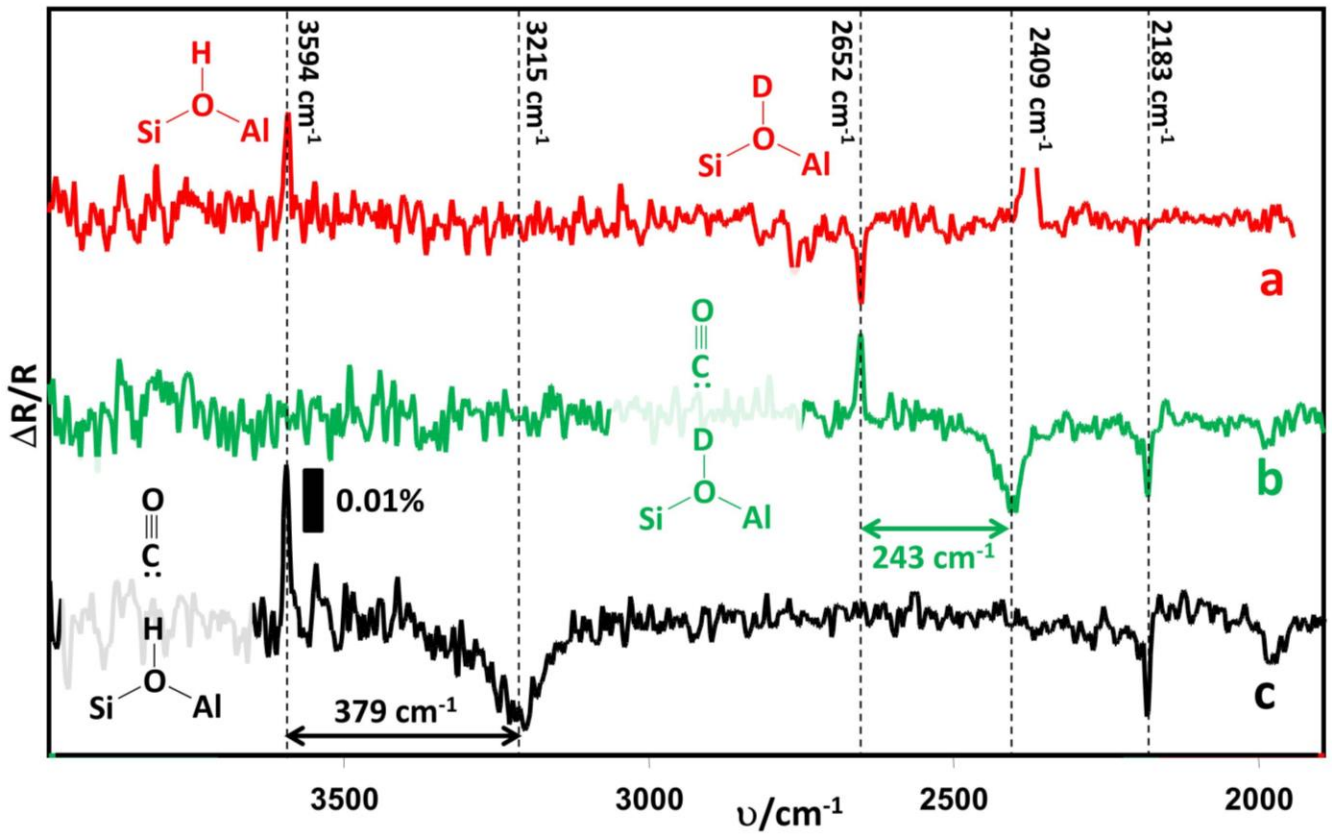

Figure 4. IRA spectra of the $Al_{0.4}Si_{0.6}O_2$ films. (a) Film with bridging OH groups (3594 cm^{-1}) subjected to H/D exchange (new OD_{br} feature at 2652 cm^{-1}) by exposure to D_2O; the difference spectrum before and after the exchange is shown. (b) and (c) correspond to films with bridging OD and OH groups recorded in 2×10^{-5} mbar CO atmosphere at 100 K, respectively. Spectra (b) and (c) are referenced to the surface before CO exposure, giving the corresponding shifted peaks OD_{br} at 2409 cm^{-1} and OH_{br} at 3215 cm^{-1}. Additionally, a peak is seen at 2183 cm^{-1} corresponding to the CO vibration in the complex, which is blue-shifted 40 cm^{-1} from gas phase CO. Figure adapted from ref. [17].

Figure 5

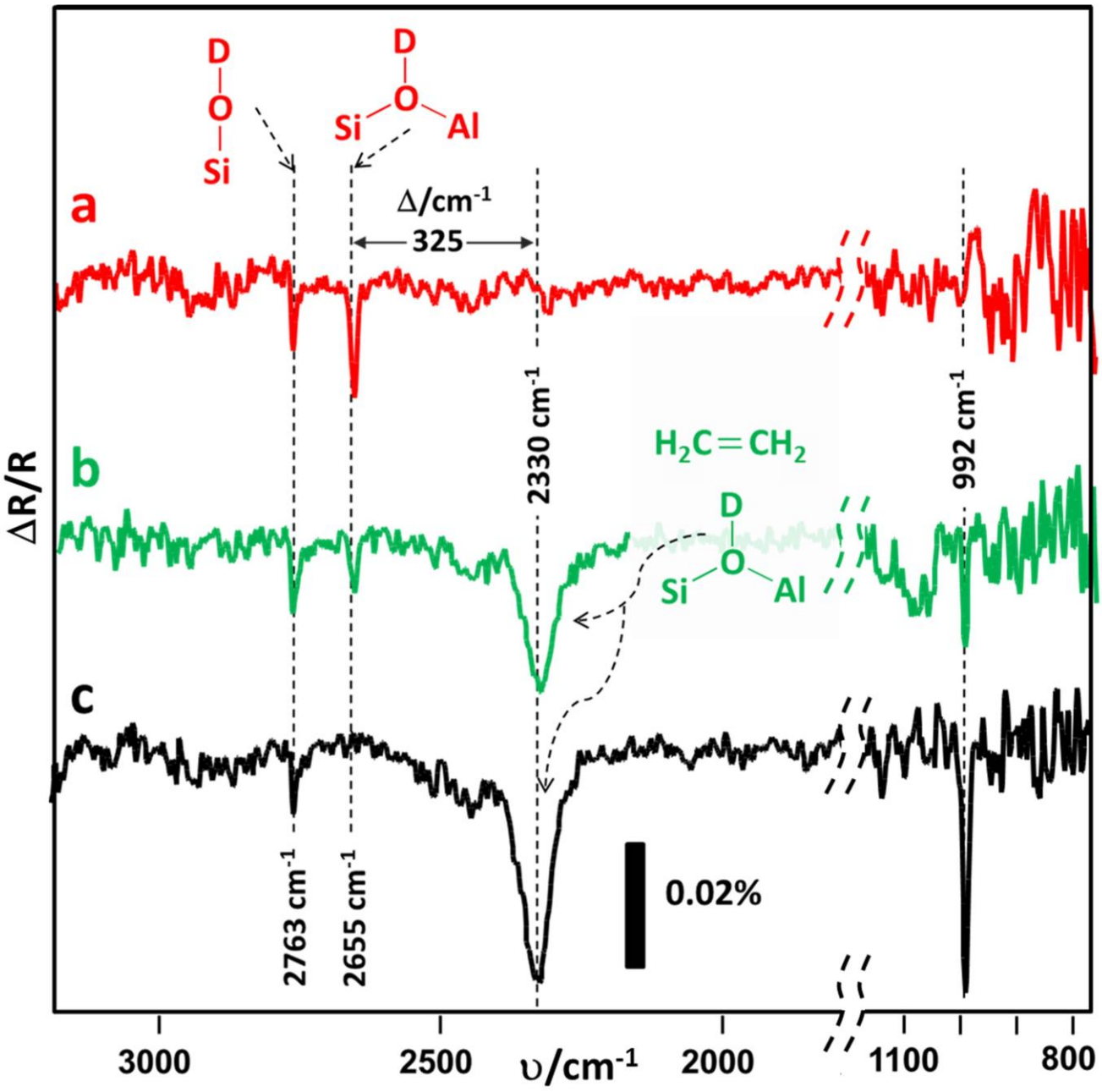

Figure 5. IRA spectra of a film with bridging OD (2655 cm^{-1}) groups and d-silanol (2763 cm^{-1}) groups (a) before dosing ethene, and (b) and (c) after increasing doses of C_2H_4. (b) and (c) show the shift in the OD_{br} (to 2330 cm^{-1}) upon dosing C_2H_4. The CH wagging mode from C_2H_4 is also evident in the spectra. Figure adapted from ref. [19].

Figure 6

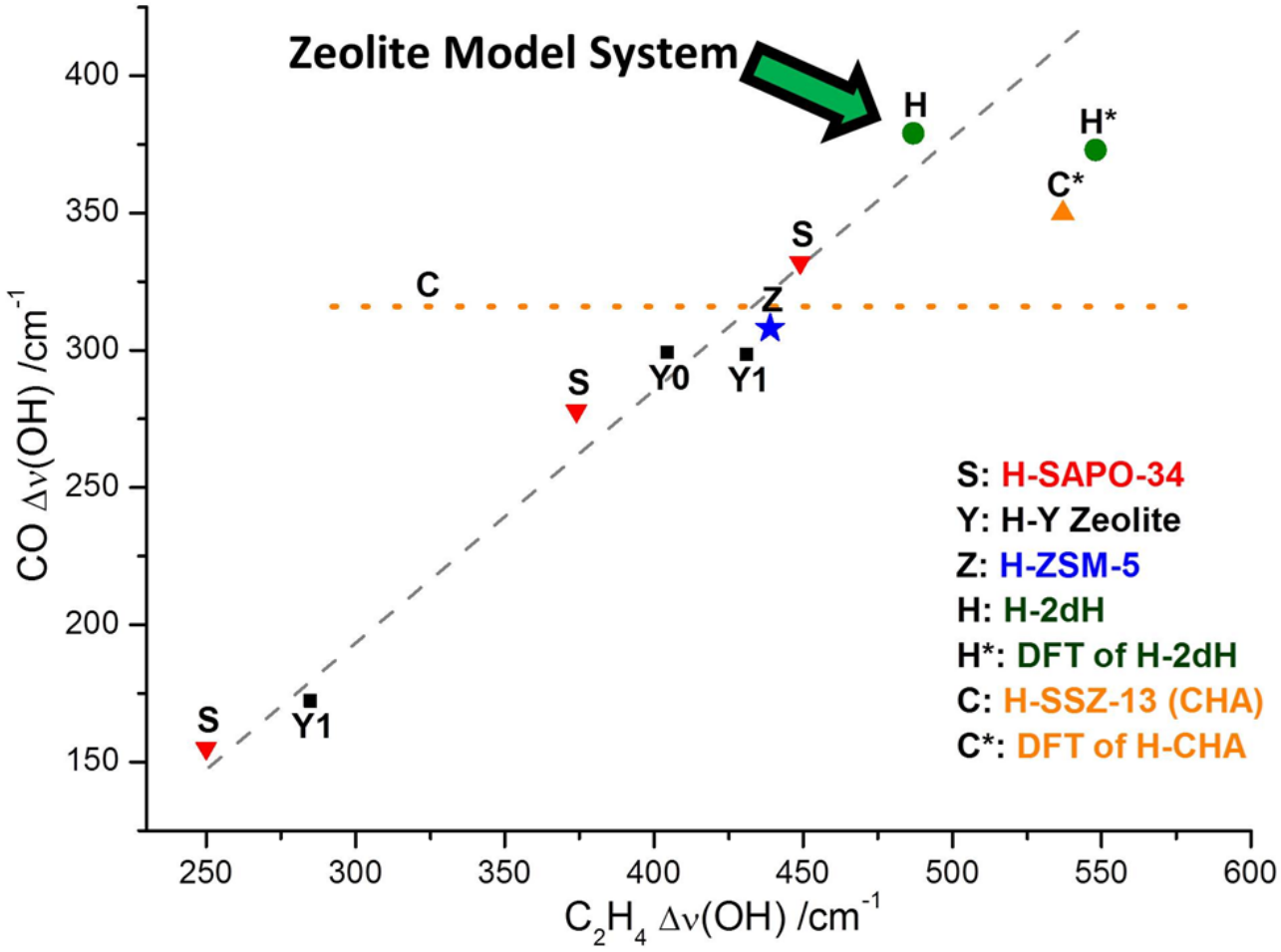

Figure 6. Plot of shifts in the OH vibration induced by C_2H_4 (x-axis) and CO (y-axis) for a variety of zeolites and zeotypes, including the film reported in this work (H, green circle). Figure adapted from ref. [19]

Figure 7

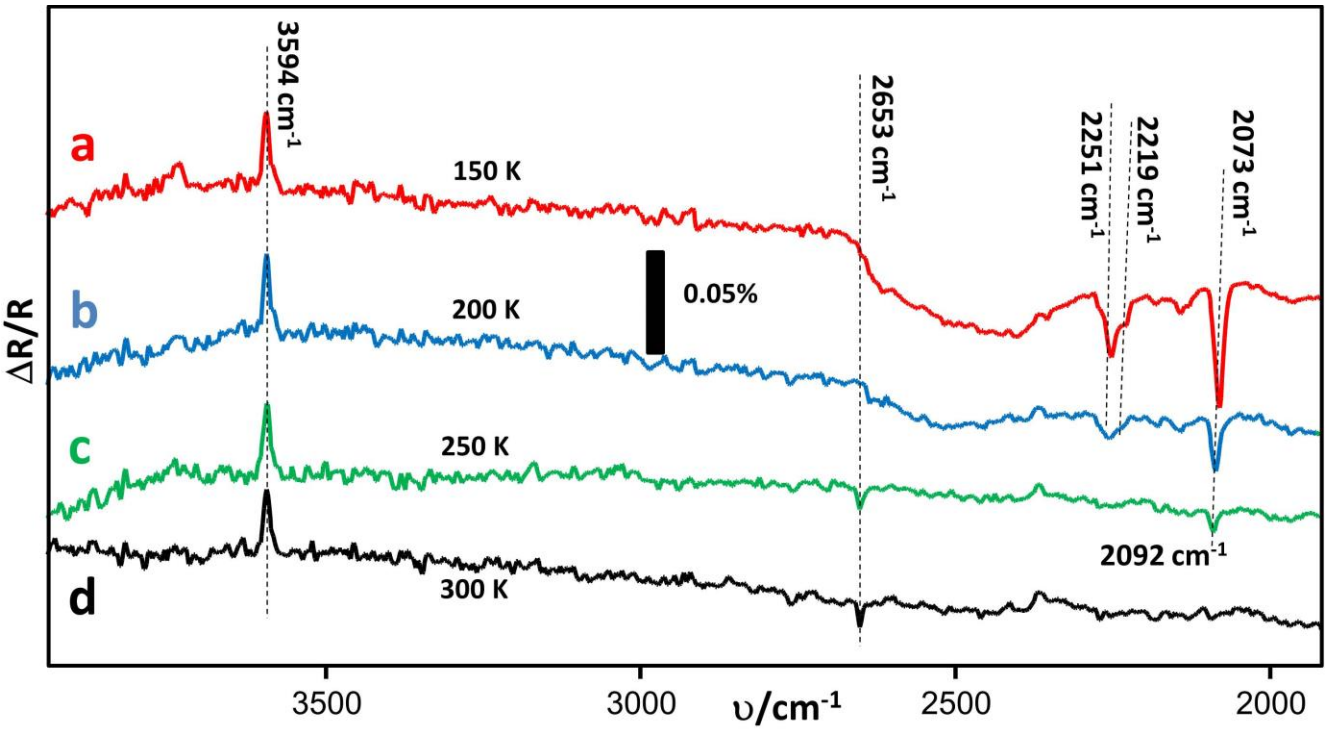

Figure 7. Spectra of d4-methanol adsorbed on bridging OH groups, referenced to a spectrum taken before d4-methanol adsorption, taken after heating to the temperatures shown with each spectrum. The peak at 3594 cm^{-1} (a-d) corresponds to the consumed bridging OH groups. The peak at 2653 cm^{-1} corresponds to the bridging OD groups formed upon H/D exchange (c-d). The broad feature between 2300 cm^{-1} and 2600 cm^{-1} results from hydrogen bonded OD groups and the peaks at 2251 cm^{-1}, 2219 cm^{-1} and 2073 cm^{-1} correspond to C—D vibrations in d4-methanol.